Assisted Prediction of Hypertension Based on Heart Rate Variability and Improved Residual Networks

Yong Zhao, Jian He, Cheng Zhang

Abstract—Cardiovascular disease resulting from hypertension poses a significant threat to human health, and early detection of hypertension can potentially save numerous lives. Traditional methods for detecting hypertension require specialized equipment and are often incapable of capturing continuous blood pressure fluctuations. To address this issue, this study starts by analyzing the principle of heart rate variability (HRV) and introduces the utilization of sliding window and power spectral density (PSD) techniques to analyze both temporal and frequency domain features of HRV. Subsequently, a hypertension prediction network that relies on HRV is proposed, combining Resnet, attention mechanisms, and a multi-layer perceptron. The network leverages a modified ResNet18 to extract frequency domain features, while employing an attention mechanism to integrate temporal domain features, thus enabling auxiliary hypertension prediction through the multi-layer perceptron. The proposed network is trained and tested using the publicly available SHAREE dataset from PhysioNet. The results demonstrate that the network achieves a high prediction accuracy of 92.06% for hypertension, surpassing traditional models such as K Near Neighbor (KNN), Bayes, Logistic regression, and traditional Convolutional Neural Network (CNN).

Keywords—Feature extraction, heart rate variability, hypertension, residual networks.

I. Introduction

WITH the continuous improvement of living conditions and the enhancement of quality of life, many chronic diseases have gradually emerged as invisible killers of physical health. Although these chronic diseases can be effectively managed, their complications pose a greater risk to people's health overall [1]. Due to changes in lifestyle and work patterns in our country, unhealthy habits such as staying up late, excessive drinking, and smoking have led to an increasing number of people suffering from chronic non-communicable diseases, including hypertension. These diseases have become significant public health issues in China. According to the China Cardiovascular Health and Disease Report 2020 published in July 2021, cardiovascular diseases caused by hypertension rank first among the causes of death for both urban and rural residents in China, surpassing other diseases.

There are two main methods for monitoring hypertension: direct blood pressure measurement and indirect measurement using the Korotkoff sound method. Direct measurement is invasive and involves inserting a catheter into a peripheral artery, while the Korotkoff sound method [2] is non-invasive and uses a cuff and stethoscope to detect arterial sounds. Both methods have limitations such as external noise interference

and variations in pulse strength among individuals, which can affect accuracy. Additionally, the Korotkoff sound method may not be suitable for long-term and continuous monitoring.

During the process of heartbeating, the human body undergoes a series of electrophysiological changes. These changes generate electrical signals that can be picked up from the body surface using electrodes, and they are continuously displayed on a timeline to form an electrocardiogram (ECG) [3]. Researchers have found that the interactions between the sympathetic and parasympathetic nervous systems in the autonomic nervous system (ANS) [4], [5] of the human body affect the rhythmicity of heartbeats and result in small variations over time, known as heart rate variability (HRV). HRV is one of the non-invasive indicators that has gained attention in recent years for cardiac monitoring. Analyzing HRV can indirectly quantitatively evaluate the tension and balance of cardiac sympathetic and vagal nerves, as well as analyze the activity of the autonomic nervous system [6]–[8]. For example, HRV can serve as an independent predictor for the risk of sudden cardiac death [9]. Abrishami et al. [10] proposed an expert system for assisting hypertension detection based on a multi-layer neural network. The system takes inputs such as patient's systolic blood pressure, smoking status, age, weight, and body mass index (BMI), and predicts the diagnosis of hypertension using the multi-layer neural network. The experiment achieved good results. Ren et al. [11] used LSTM to classify textual sequences in electronic medical records and combined an autoencoder to classify numerical data in electronic medical records. The outputs of the two classifiers were then merged into a fully connected layer, and the model predicted renal diseases in hypertension patients using Softmax classification. The effectiveness of the model was validated through experiments and comparisons with other algorithms. Some researchers have conducted hypertension prediction by extracting feature parameters of HRV and combining them with machine learning algorithms. For example, Wang et al. [12] developed a prediction model for hypertension based on logistic regression and artificial neural networks without measurement. They used binary logistic regression to predict the significant risk factors leading to hypertension. The experimental results showed an accuracy of over 72% for the model. Pavithran et al. analyzed HRV and other conventional parameters (including HRV during deep breathing, blood pressure response during static standing, and isometric grip strength) in 35 male subjects. The experimental results showed that the parasympathetic function of hypertension patients was impaired, leading to a decrease in HRV compared to the normal population [13],

Yong Zhao is with Beijing University of Technology, China (corresponding author, phone: (+86)18735724319; e-mail: 1030678904@qq.com).

Jian He is a professor and Cheng Zhang is a PhD student at the Department of Information Science at Beijing University of Technology.

World Academy of Science, Engineering and Technology
International Journal of Computer and Information Engineering
Vol:18, No:1, 2024

[14]. In general, there is currently a lack of deep learning based hypertension prediction techniques specifically targeting HRV. Lan et al. [15] used intelligent wearable devices to collect continuous 6-hour photoplethysmography (PPG) signals from 24 hypertension patients and 19 healthy individuals. They extracted six HRV features and achieved an 85.47% accuracy rate for hypertension classification. However, the accuracy of hypertension prediction using PPG signals is affected by the fact that PPG waveforms do not carry important high-frequency components and are highly sensitive to motion artifacts [16]. Therefore, in this study, the HRV features of hypertension patients are analyzed using ECG signals, and deep learning algorithms are combined to study hypertension prediction techniques based on HRV.

The rest of the paper is structured as follows: In Section II, a comparative analysis is conducted between the heart rate variability (HRV) of normal individuals and that of individuals with hypertension. A sliding window and PSD are introduced to analyze the time-domain and frequency-domain features of HRV. In Section III, a hypertension prediction network is presented based on HRV, which integrates ResNet18, attention mechanisms, and multi-layer perceptron. The network extracts frequency-domain features from PSD graphs and combines them with time-domain features through attention mechanisms. The multi-layer perceptron is then used for hypertension classification prediction. In Section IV, the SHAREE [17] dataset is used for network training and experiments, and the hypertension prediction results of the proposed model are compared with those of traditional machine learning algorithms. Finally, a summary is provided in the conclusion of the paper.

II. RELATED WORK

The methods for analyzing HRV mainly include time-domain analysis and frequency-domain analysis [18]–[20]. In this section, based on the analysis of HRV features in hypertensive patients, a sliding window and PSD technique are introduced to transform the ECG data into time-frequency domain features. This provides a foundation for the subsequent construction of an improved residual network for hypertension-assisted prediction.

A. Analysis of HRV in Hypertensive Patients

Due to the elevation of blood pressure, changes such as vasodilation and accelerated heart rate may occur. Therefore, extracting the HRV features by analyzing the heart rate interval sequence based on electrocardiogram (ECG) is a necessary step for assisting in predicting hypertension. Fig. 1 compares the heart rate interval images between normal individuals and hypertensive patients. The horizontal axis represents the heart rate interval sequence within one minute, and the vertical axis represents the time difference between the current and previous heartbeats. The heart rate interval sequence with a relatively flat curve represents normal individuals, with a mean time difference of 886.12 and a heart rate of 68 beats per minute. The heart rate interval sequence with more fluctuations represents hypertensive patients, with a mean time

difference of 793.54 and a heart rate of 77 beats per minute. Compared with normal individuals, hypertensive patients have lower HRV values. Based on the differences in HRV between healthy individuals and hypertensive patients, analysis of the time-frequency domain features of HRV provides a foundation for subsequent research.
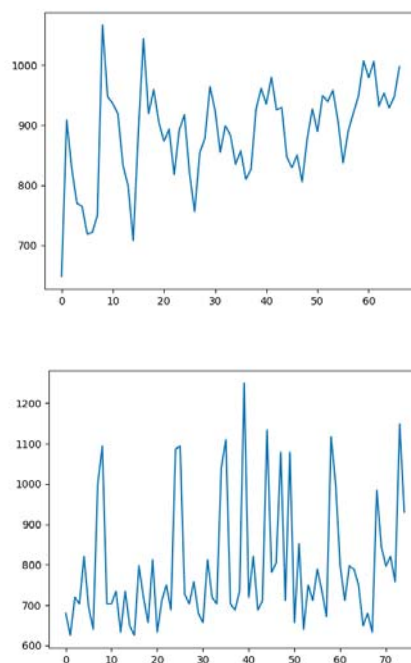
Fig. 1 Heartbeat interval diagram

B. HRV Time-Frequency Domain Characterization

ECG data, often collected by instrument equipment, are susceptible to irregularities caused by factors such as breathing and movement, resulting in missing data points and noise that can affect subsequent analysis. To extract HRV features accurately, it is necessary to obtain a feature vector as a standard for assisted prediction. Firstly, the original ECG data are sampled using a cubic spline interpolation to improve the time accuracy of peak detection. Secondly, a high-pass Butterworth filter is applied to reduce potential long-term drift in the signal. Finally, a Savitzky-Golay filter is used to smooth the data, reducing sharp peaks while maintaining time accuracy.

After pre-processing the raw data, it is necessary to extract time-frequency domain features from the processed data. Due to the continuous and long-term nature of ECG data, traditional analysis methods for static data are insufficient for this scenario. Therefore, this paper utilizes a sliding window technique. As shown in Fig. 2, a window of 20 seconds is used to cache ECG data and perform wave detection and feature analysis of each window of ECG data, with corresponding timestamps set to save the time-frequency domain feature results. As new data are continuously generated, the sliding

World Academy of Science, Engineering and Technology
International Journal of Computer and Information Engineering
Vol:18, No:1, 2024
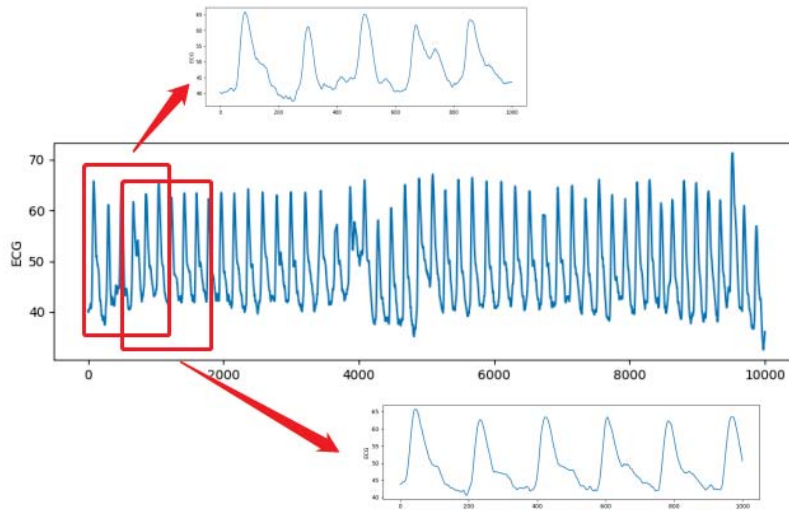
Fig. 2 Sliding window to extract features

window updates its data according to the first in first out rule and continuously saves its analysis results.

For ECG data, peak detection can be influenced by unrelated prominent P-waves and T-waves. Specifically, traditional amplitude-based analysis may occasionally detect non-R-wave peaks that have similar or larger amplitudes compared to the R-wave. Therefore, for ECG data, K-means clustering is applied to differentiate R-waves from the commonly present P and T waves in the signal, followed by the extraction of the RR interval sequence.

The RR interval sequence, which has been extracted, is initially subjected to time-domain signal analysis to extract its time-domain feature parameters. The primary parameters in focus include RR, Standard Deviation of Normal-to-Normal intervals (SDNN), Root Mean Square of Successive Differences (RMSSD), and Percentage of RR intervals greater than 50ms in total RR intervals(PNN50), as described in Table I.

TABLE I
TIME DOMAIN CHARACTERISTICS

Features	Feature Description
RR(Mean)	RR interval mean
SDNN	RR Standard deviation of continuous normal RR interval
RMSSD	The root mean square of the difference between adjacent R-R intervals
PNN50	RR The number of adjacent normal R-R intervals with a difference greater than 50ms as a percentage of the total number of heartbeats

Subsequently, the frequency-domain feature parameters for heart rate variability are extracted from the PSD estimation. Fourier Transform is used to convert the signal from the time-domain to the frequency-domain. Its formula is shown in (1), where f represents the frequency component of x, and t represents time. The equation can be understood as the time-domain signal $x(t)$ being multiplied by an exponential term consisting of specified frequencies ($e^{-2\pi i f t}$). The integral of this product over the entire time axis produces the frequency-domain signal, which identifies the spectral components of the signal. PSD is defined as the square of the modulus of the Fast Fourier Transform and is expressed as (2). The power spectrum reflects the changes in signal power with frequency in a given frequency band, i.e. the distribution of signal power in the frequency-domain.

$$S(f) = \int_{-\infty}^{+\infty} x(t) * e^{-2\pi i f t} dt \qquad (1)$$

$$P = \lim_{T \to \infty} \frac{1}{T} \int |S(f)|^2 df \qquad (2)$$

The raw ECG data, represented as a one-dimensional signal, are converted into a three-channel RGB image using PSD. This image incorporates frequency-domain features of heart rate intervals within a sliding window. The utilization of this image provides a foundation for exploring high blood pressure prediction techniques based on an improved residual network.

III. METHOD

In this section, we first introduce a network architecture that integrates Resnet [21], attention mechanism, and multilayer perceptron. Secondly, we provide an overview of the principles of Resnet and the extraction of frequency-domain features using the improved Resnet18. Lastly, we discuss the fusion of time-frequency domain feature vectors based on attention mechanism.

A. Network Architecture

The preprocessed ECG data are transformed into individual RGB images through the utilization of sliding windows and PSD conversion. These images can be subjected to feature extraction using convolutional networks. Building upon the analysis and comparison of traditional convolutional networks such as KNN [22], Bayes [23], Logistic [24], and CNN [25], this paper introduces a network architecture that integrates Resnet, attention mechanism, and multilayer perceptron (as depicted in Fig. 3). This architecture comprises of an input

World Academy of Science, Engineering and Technology
International Journal of Computer and Information Engineering
Vol:18, No:1, 2024

layer, Resnet layer, fusion layer, fully connected layer, and softmax layer.

The input layer receives RGB images and feeds them into the Resnet layer. The ResNet layer consists of multiple convolutional blocks and residual blocks to extract frequency-domain features from the images. The fusion layer utilizes attention mechanism to fuse the frequency-domain feature vectors with the time-domain feature vectors. Finally, the feature vectors are classified through the fully connected layer (which is essentially a multilayer perceptron) and softmax layer. The predicted result is determined by selecting the class with the highest probability and is then outputted.

B. Resnet-Based Frequency Domain Feature Extraction

ResNet proposed the residual learning method to alleviate the difficulties of training deep neural networks, which often leads to a decrease in accuracy. As shown in Fig. 4, each residual module contains two paths, one of which is a direct path to the input feature, while the other path applies two to three convolutional operations to the feature to obtain the residual feature F(x), with both paths having their own weights. Finally, the two results are added together as input for the next layer. If the convolutional path does not produce good results, its weight is set to zero, resulting in the input being treated as an identity mapping, ensuring that the effect is no worse than that of the original input. The addition of residual modules can avoid the problem of gradient disappearing, further improving the fitting ability of the model and reducing the impact of increasing network depth.

The improved Resnet18 mainly includes an input layer, several intermediate layers, and an average pooling layer, as shown in Fig. 5. The input layer consists of a convolutional layer and a max pooling layer. The intermediate layers, indicated by the dotted lines in the figure, consist of four convolutional blocks containing residual modules, followed by an average pooling layer to output the feature values.

The input, which is transformed by PSD (Position-Specific Discrete) convolution, has a size of 224*224*3. It consists of three channels, each with a size of 224*224. This input includes a convolutional layer with a 7*7 kernel and a stride of 2, as well as a 3*3 max pooling layer with a stride of 2. Through this process, the image is reduced to a feature map of size 56*56, significantly reducing the required storage space. In the intermediate layers, there are a total of four convolutional blocks. The convolutional layer is a crucial component of the CNN as it is responsible for extracting features from the raw data while preserving the spatial continuity of the image. It captures local features of the data, and the convolutional kernel has parameter-sharing capabilities, effectively reducing the number of parameters in the convolutional layer. Firstly, the input passes through a convolutional layer with a 3*3 kernel, a stride of 2, padding of 1, and an output channel of 64. The output of this layer is 64*112*112. Secondly, it goes through another convolutional layer with a 3*3 kernel, a stride of 1, padding of 1, and an output of 128*56*56. Finally, there are two 11 convolutional layers and one downsampling operation. Each layer has a

stride of 2, padding of 1, and doubles the output channels while halving the size of the output vector. The final output vector has a size of 512*7*7. It then undergoes average pooling, resulting in an output vector of size 512*1*1.

C. Attention-Based Mechanism for Time-Frequency Domain Feature Fusion

To begin with, the frequency-domain feature vectors generated by the ResNet layer and the time-domain feature vectors obtained through computation are utilized together as inputs for the attention mechanism. Then, a scoring function is employed to compute the correlation between the query vector q and each input vector, resulting in a score. The higher the score, the higher the weight. The feature vectors are then weighted and concatenated using the concat function. Finally, the classification results are output through a fully connected layer and softmax layer. The scoring function is defined by (3), where x represents the query, x_i represents the key, and y_i represents the value corresponding to the key. The attention weight between query x and key x_i is denoted by $\propto (x, x_i)$, and if a key is closer to the given query x, a larger attention weight is assigned to its corresponding value y_i.

$$\mathbf{f}(\mathbf{x}) = \sum_{i=1}^{n} \propto (x, x_i) y_i \qquad (3)$$

IV. EXPERIMENTAL DESIGN AND ANALYSIS OF RESULTS

A. Experimental Data Set

The dataset used in this study is derived from the publicly available dataset of SHAREE. The dataset was developed for studying the possibility of identifying subjects at risk of cardiovascular events based on heart rate variability analysis. The data include information such as electrocardiogram data and basic patient information, totaling 1260 cases, of which 139 cases are hypertension patients, and the remaining are healthy individuals. Hypertension is commonly seen in middle-aged and elderly populations. In this dataset, the age of hypertension patients is concentrated in the range of [60-70] years, with an average age of 71.76 years. In machine learning, in order to reflect the generalization performance of algorithms, three-quarters of the dataset is randomly selected as training samples, and the rest are used as test samples. A binary classification model is established using the presence or absence of hypertension symptoms as the label result. To evaluate the effectiveness of the hypertension prediction model, it is necessary to assess its predictive performance. In this study, the model is evaluated from three dimensions: accuracy, recall rate, and AUC (Area Under the Curve).

(1) Accuracy: The accuracy of predicting the presence or absence of hypertension is measured as shown in (4), where TP represents the number of true positives (correctly predicted hypertensive patients), TN represents the number of true negatives (correctly predicted non-hypertensive patients), FN represents the number of false negatives (incorrectly predicted hypertensive patients), and FP represents the number of false positives (incorrectly predicted non-hypertensive patients).

World Academy of Science, Engineering and Technology
International Journal of Computer and Information Engineering
Vol:18, No:1, 2024
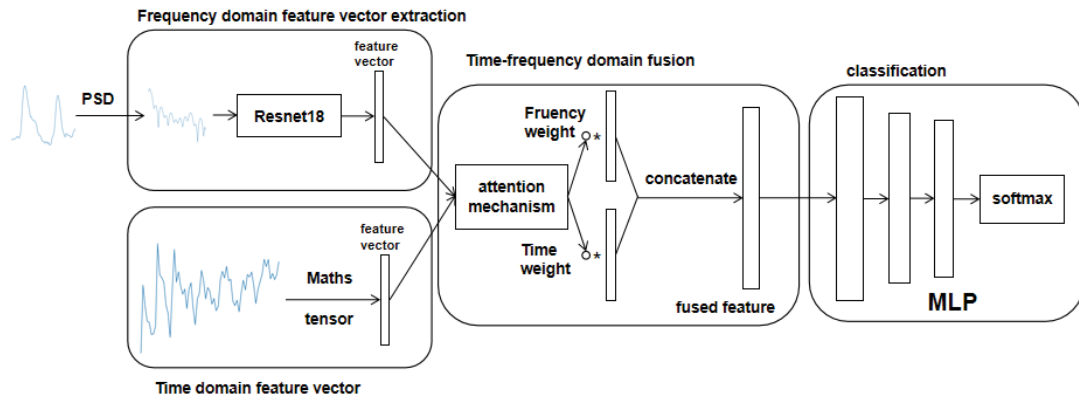
Fig. 3 Network architecture diagram
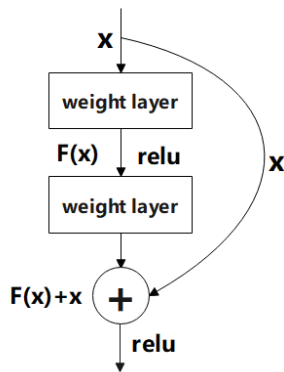
Fig. 4 Residual unit
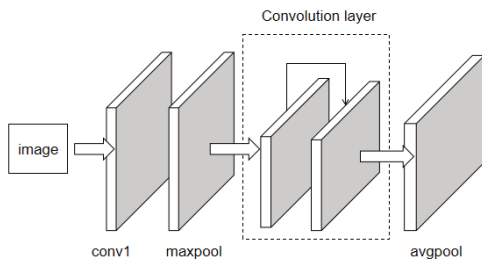
Fig. 5 Resnet18 architecture

$$accuracy = \frac{TP + TN}{TP + FN + FP + TN} \quad (4)$$

(2) Recall: The proportion of correctly predicted hypertensive patients among all hypertensive patients in the sample set is represented as shown in (5):

$$recall = \frac{TP}{TP + FN} \quad (5)$$

(3) F1 value: It is an evaluation metric that combines Precision and Recall, aiming to provide a comprehensive representation of the overall performance. The formula for this metric is shown as (6):

$$F1 = \frac{2 * accuracy * recall}{accuracy + recall} \quad (6)$$

B. Analysis of Results

To validate the impact of data preprocessing, two comparative experiments were conducted in the early stage of this study using an improved residual network. One experiment utilized preprocessed data, while the other experiment used raw, unprocessed data. The results are presented in Table II. The results demonstrate the necessity of preprocessing the raw data before using it for analysis.

TABLE II
COMPARISON OF DATA PRE-PROCESSING

Testing	Pre-processing	Not pre-processed
Accuracy	91.03	82.7
Recall Rate	93.46	84.28
F1	0.91	0.83

Next, the preprocessed data were fed into the model for testing, and the results were obtained by averaging the outcomes over 10 trials, as shown in Table III. The average accuracy of the ten classification predictions was found to be 92.06%, with an average recall of 93.55% and an average F1 score of 0.92.

TABLE III
CLASSIFICATION PREDICTION RESULTS BASED ON RESNET18

Testing	Accuracy/%	Recall/%	F1
TEST1	90.03	99.87	0.95
TEST2	93.46	98.28	0.96
TEST3	94.10	97.90	0.95
TEST4	91.30	83.25	0.87
TEST5	90.57	83.76	0.87
TEST6	89.73	96.85	0.93
TEST7	91.52	94.63	0.93
TEST8	95.81	97.82	0.96
TEST9	91.57	92.67	0.92
TEST10	92.51	90.44	0.91
Average	92.06	93.55	0.92

To validate the effectiveness of the proposed network model, it was compared with the KNN, Bayes, Logistic, and CNN

algorithms. In the K-NN algorithm, the value of k was set to 2. The Bayes algorithm implements the principle of conditional probability to determine the probability after events are exchanged. Logistic classification is a supervised learning approach that requires manual annotation. CNN represents the traditional convolutional neural network. All four classification algorithms were evaluated using the same data, with the same training and testing lengths. The performance evaluation results averaged over 10 runs, are presented in Table IV. It can be observed that the average performance of the Bayes algorithm is significantly lower than the other four algorithms. This could be attributed to the strong assumption of independence between features in Bayes' law, neglecting the inter-dependencies among features. The KNN, Logistic, and CNN algorithms achieved an average accuracy of around 70-80%. In contrast, the proposed residual network exhibited the highest average accuracy at approximately 92% and also attained the highest F1 score of 0.92.

TABLE IV
PREDICTION RESULTS OF DIFFERENT ALGORITHMS

Classification Algorithm	Accuracy/%	Recall/%	F1
KNN	79.84	77.21	0.79
Bayes	49.44	39.28	0.44
Logistic	76.92	80.42	0.77
CNN	88.64	82.38	0.85
Resnet18	92.06	93.55	0.92

Finally, this study compared the effect of the number of layers in a multilayer perceptron on accuracy. The parameters and training data were kept consistent with the previous experiments, while the number of layers in the multilayer perceptron was increased or decreased, solely for the purpose of observing the classification performance of different numbers of layers. The results of this analysis are presented in Table V.

TABLE V
ACCURACY RATE OF DIFFERENT LAYERS

Number of layers	Accuracy/%	Recall/%	F1
2	89.48	90.25	0.89
3	92.06	93.55	0.92
4	88.26	87.35	0.87

When there are only 2 layers, it may not be able to comprehensively extract and refine the features, resulting in low accuracy. On the other hand, when there are 4 layers, it may lead to overfitting of the features and also result in lower accuracy. Therefore, in this study, a multilayer perceptron with 3 layers was selected as the optimal configuration.

V. CONCLUSION

Due to the lack of obvious early symptoms of hypertension, patients themselves find it difficult to detect the condition. This study aims to provide precise early warning and prediction of hypertension risk to individuals with minimal economic and physical burden. The main focus of this paper is to propose a hypertension-assistant prediction model based on the fusion of HRV time-frequency domain features, residual networks, attention mechanisms, and multilayer perceptrons. Experimental comparisons were conducted using the publicly available SHAREE dataset. The results demonstrate that the proposed model outperforms the other four classification algorithms in assisting hypertension prediction. It provides clearer and more accurate guidance and support for healthcare professionals, thus aiding further examinations. Future work will involve adjusting the network structure, including the number of convolutional layers and the size of convolutional kernels. Additionally, continuous optimization of model parameters and exploration of more model fusion techniques will be pursued.

REFERENCES

[1] C. Troeger, M. Forouzanfar, P. C. Rao, I. Khalil, A. Brown, R. C. Reiner, N. Fullman, R. L. Thompson, A. Abajobir, M. Ahmed *et al.*, "Estimates of global, regional, and national morbidity, mortality, and aetiologies of diarrhoeal diseases: a systematic analysis for the global burden of disease study 2015," *The Lancet infectious diseases*, vol. 17, no. 9, pp. 909–948, 2017.

[2] A. Meidert, J. Briegel, and B. Saugel, "Principles and pitfalls of arterial blood pressure measurement," *Der Anaesthesist*, vol. 68, pp. 637–650, 2019.

[3] P. Lamba and K. Rawal, "A survey of algorithms for feature extraction and feature classification methods," in *2019 International Conference on Automation, Computational and Technology Management (ICACTM)*. IEEE, 2019, pp. 338–341.

[4] C. M. van Ravenswaaij-Arts, L. A. Kollee, J. C. Hopman, G. B. Stoelinga, and H. P. van Geijn, "Heart rate variability," *Annals of internal medicine*, vol. 118, no. 6, pp. 436–447, 1993.

[5] J. P. ZBILUT and L. LAWSON, "Decreased heart rate variability in significant cardiac events," *Critical care medicine*, vol. 16, no. 1, pp. 64–66, 1988.

[6] G. Wilson, "A review of "the polyvagal theory: Neurophysiological foundations of emotions, attachment, communication, and self regulation" stephen w. porges.(2011). new york: Ww norton, 272 pp., $45.00 (hardback)." 2012.

[7] B. Folkow, "Physiological aspects of primary hypertension." *Physiological reviews*, vol. 62, no. 2, pp. 347–504, 1982.

[8] S. Oparil, "The sympathetic nervous system in clinical and experimental hypertension," *Kidney international*, vol. 30, no. 3, pp. 437–452, 1986.

[9] B. Xhyheri, O. Manfrini, M. Mazzolini, C. Pizzi, and R. Bugiardini, "Heart rate variability today," *Progress in cardiovascular diseases*, vol. 55, no. 3, pp. 321–331, 2012.

[10] Z. Abrishami and H. Tabatabaee, "Design of a fuzzy expert system and a multi-layer neural network system for diagnosis of hypertension," *Bull Environ Pharmacol Life Sci*, vol. 4, no. 11, pp. 138–145, 2015.

[11] Y. Ren, H. Fei, X. Liang, D. Ji, and M. Cheng, "A hybrid neural network model for predicting kidney disease in hypertension patients based on electronic health records," *BMC medical informatics and decision making*, vol. 19, pp. 131–138, 2019.

[12] A. Wang, N. An, G. Chen, L. Li, and G. Alterovitz, "Predicting hypertension without measurement: A non-invasive, questionnaire-based approach," *Expert Systems with Applications*, vol. 42, no. 21, pp. 7601–7609, 2015.

[13] P. Pavithran, M. Madanmohan, R. Mithun, M. Jomal, and H. Nandeesha, "Heart rate variability in middle-aged men with new-onset hypertension," *Annals of Noninvasive Electrocardiology*, vol. 13, no. 3, pp. 242–248, 2008.

[14] A. Gunther, I. Salzmann, S. Nowack, M. Schwab, R. Surber, H. Hoyer, O. Witte, and D. Hoyer, "Heart rate variability–a potential early marker of sub-acute post-stroke infections," *Acta neurologica Scandinavica*, vol. 126, no. 3, pp. 189–196, 2012.

[15] K.-c. Lan, P. Raknim, W.-F. Kao, and J.-H. Huang, "Toward hypertension prediction based on ppg-derived hrv signals: A feasibility study," *Journal of medical systems*, vol. 42, pp. 1–7, 2018.

[16] K. M. Warren, J. R. Harvey, K. H. Chon, and Y. Mendelson, "Improving pulse rate measurements during random motion using a wearable multichannel reflectance photoplethysmograph," *Sensors*, vol. 16, no. 3, p. 342, 2016.

World Academy of Science, Engineering and Technology
International Journal of Computer and Information Engineering
Vol:18, No:1, 2024

[17] PhysioNet, https://www.physionet.org/content/shareedb.
[18] H. Kawano, R. Okada, and K. Yano, "Histological study on the distribution of autonomic nerves in the human heart," *Heart and vessels*, vol. 18, no. 1, p. 32, 2003.
[19] J. L. Hamilton and L. B. Alloy, "Atypical reactivity of heart rate variability to stress and depression across development: Systematic review of the literature and directions for future research," *Clinical psychology review*, vol. 50, pp. 67–79, 2016.
[20] C. Schiweck, D. Piette, D. Berckmans, S. Claes, and E. Vrieze, "Heart rate and high frequency heart rate variability during stress as biomarker for clinical depression. a systematic review," *Psychological medicine*, vol. 49, no. 2, pp. 200–211, 2019.
[21] K. He, X. Zhang, S. Ren, and J. Sun, "Deep residual learning for image recognition," in *Proceedings of the IEEE conference on computer vision and pattern recognition*, 2016, pp. 770–778.
[22] A. M. Alsayat, "Efficient genetic k-means clustering algorithm and its application to data mining on different domains," Ph.D. dissertation, Bowie State University, 2016.
[23] D. Niedermayer, "An introduction to bayesian networks and their contemporary applications," *Innovations in Bayesian networks: Theory and applications*, pp. 117–130, 2008.
[24] C.-c. Chen, K. Mondal, P. Vervliet, A. Covaci, E. P. O'Brien, K. J. Rockne, J. L. Drummond, and L. Hanley, "Logistic regression analysis of lc-ms/ms data of monomers eluted from aged dental composites: A supervised machine-learning approach," *Analytical Chemistry*, 2023.
[25] A. Roslin, M. Lebedev, T. Mitchell, I. Onederra, and C. Leonardi, "Processing of micro-ct images of granodiorite rock samples using convolutional neural networks (cnn). part iii: Enhancement of scanco micro-ct images of granodiorite rocks using a 3d convolutional neural network super-resolution algorithm," *Minerals Engineering*, vol. 195, p. 108028, 2023.